Two-gap features in the specific heat of (M,K)Fe_{2}As_{2} (M = Ba, Sr)

F. Y. Wei, B. Lv, Y. Y. Xue, and C. W. Chu

Phys. Rev. B **84**, 064508 — Published 18 August 2011

DOI: 10.1103/PhysRevB.84.064508

Two-Gap Features in the Specific Heat of $(M,\mathrm{K})\mathrm{Fe_2As_2}$ with M = Ba, Sr

F. Y. Wei,[1] B. Lv,[1] Y. Y. Xue,[1] and C. W. Chu[1,2]

[1]Department of Physics and TCSUH, University of Houston, Houston, Texas 77204-5002, USA

[2]Lawrence Berkeley National Laboratory, 1 Cyclotron Road, Berkeley, California 94720, USA

ABSTRACT

The specific heat coefficient C_p / T was investigated for the optimally doped $\mathrm{Ba_{0.6}K_{0.4}Fe_2As_2}$ and $\mathrm{Sr_{0.55}K_{0.45}Fe_2As_2}$. Previously, both the single and the two-gap pairing have been suggested for $\mathrm{Ba_{0.6}K_{0.4}Fe_2As_2}$ single crystals. Our analysis reveals that the controversy is mainly caused by the differences in the adopted phonon background. This is especially true in the $(\mathrm{Ba,K})\mathrm{Fe_2As_2}$ system, where the phonon contribution below 20 K significantly deviates from the simplified Debye model and, in addition, strongly depends on the doping. The different pairing features reported previously can be reproduced from the same C_p / T data set if the respective phonon baselines are adopted. The soft-phonon shifts, therefore, were examined on the $(\mathrm{Ba,K})\mathrm{Fe_2As_2}$ and $(\mathrm{Sr,K})\mathrm{Fe_2As_2}$ systems, as well as the $(\mathrm{Ba_{0.6}K_{0.4}})(\mathrm{Fe,Co})_2\mathrm{As_2}$ system. The data show that although the K-Ba replacement may change the low-temperature slope $\beta = \dfrac{d\left(C_p / T\right)}{d(T^2)}$ by 50%, the effects of both K-Sr and Co-Fe replacements are much weaker. The carrier part, C_e / T, is consequently extracted for both $\mathrm{Sr_{0.55}K_{0.45}Fe_2As_2}$ and $\mathrm{Ba_{0.6}K_{0.4}Fe_2As_2}$. Two-gap features appear in both cases, but the coupling strength is much stronger for the Ba-based superconductors.

Introduction

One of the foremost issues surrounding the specific heat, C_p, of pnictides is the associated gap structure. Despite much spectroscopic data, which suggest a two-gap pairing,[1,2] the interpretations for the C_p / T observed are rather controversial. In the case of $Ba_{0.6}K_{0.4}Fe_2As_2$, for example, an early investigation reported that the data are consistent with a single-gap, *s*-wave pairing, although a lower critical field study of similar crystals indicates a two-gap structure.[3,4] Several later specific-heat works, however, seem to confirm this unusual observation.[5] Furthering the mystery, clear two-gap features have been reported in LiFeAs and $Ba(Fe_{0.925}Co_{0.075})_2As_2$, two compounds similar to the $(Ba,K)Fe_2As_2$ in question.[6,7] Preliminary evidence for the two-gap pairing in the $(Sr,K)Fe_2As_2$ system has also been reported.[8] In particular, a recent paper reported a rather prominent two-gap feature in $Ba_{0.68}K_{0.32}Fe_2As_2$.[9] It seems that either the gap structure is unusually sensitive to the sample quality or the analysis procedures need to be explored. Both $(Sr,K)Fe_2As_2$ and $(Ba,K)Fe_2As_2$ systems, therefore, are examined. While the gap features of the optimally doped $Sr_{0.55}K_{0.45}Fe_2As_2$ seem to be insensitive to the analysis procedures, the case of $Ba_{0.6}K_{0.4}Fe_2As_2$ is rather different. It may not be a coincidence that in both Refs. 7 and 9, in which a two-gap pairing was observed, the carrier contribution C_e / T was obtained based on the phonon part C_{ph} / T of the non-superconducting siblings $Ba(Fe,A)_2As_2$, where A = Co, Mn. On the other hand, in both Refs. 3 and 5, which claimed a single-gap structure, model fitting was used to extract C_{ph} / T. The C_{ph} / T of three 122 systems, *i.e.* $Sr_{1-x}K_xFe_2As_2$, $Ba_{1-x}K_xFe_2As_2$, and $(Ba_{0.6}K_{0.4})(Fe_{0.9}Co_{0.1})_2As_2$, therefore, are analyzed. The data show that the K-Ba replacement may significantly alter C_{ph} / T below 20 K, but the effects of K-Sr and Co-Fe (or Mn-Fe) replacements are relatively minor. The initial slope

$\beta = \frac{d(C_p/T)}{d(T^2)}\Big|_{T<3\mathrm{K}}$ (which should represent the phonon contribution for an *s*-wave-pairing superconductor if all gaps are wider than $0.5kT_c$), for example, is $6\cdot10^{-4}$ and $4\cdot10^{-4}$ mJ / mol K^4 for $BaFe_2As_2$ and $Ba_{0.6}K_{0.4}Fe_2As_2$, respectively. The difference between $SrFe_2As_2$ and $Sr_{0.55}K_{0.45}Fe_2As_2$, on the other hand, is less than 10%. As the result, neither the phonon-model fitting, where $C_{ph}/T \approx \beta T^2$ is implicitly assumed at low temperatures, nor the slightly modified C_{ph}/T of $Ba(Fe,A)_2As_2$ may represent the C_{ph}/T of $(Ba_{0.6}K_{0.4})Fe_2As_2$. Instead, the non-superconducting $(Ba_{0.6}K_{0.4})(Fe_{0.9}Co_{0.1})_2As_2$ offers a better choice. The C_e/T of both $Sr_{0.55}K_{0.45}Fe_2As_2$ and $Ba_{0.6}K_{0.4}Fe_2As_2$ are consequently extracted. The low-T tail of $Ba_{0.6}K_{0.4}Fe_2As_2$ is only half of that obtained using the C_{ph}/T of $Ba(Fe,A)_2As_2$ as the baseline. The data, however, still show clear two-gap features similar to those in $Sr_{0.55}K_{0.45}Fe_2As_2$. Both the superconducting $\Delta C_p/T$ jump at T_c and the α-model fitting, in addition, demonstrate that the coupling strength is much stronger in the Ba-based compound.

Methods

Several ceramic samples of $Sr_{1-x}K_xFe_2As_2$ with $x = 0$ and 0.45; $BaFe_2As_2$; $Ba_{0.6}K_{0.4}Fe_2As_2$; and $Ba_{0.6}K_{0.4}(Fe_{1-y}Co_y)_2As_2$ with $y = 0$, 0.04, 0.085, and 0.1 were synthesized from high temperature reactions of stoichiometric high-purity Ba, Sr, K, Fe, Co, and As, similar to that reported previously.[10] A few $BaFe_2As_2$ single crystals were also prepared by the self-flux method. The X-ray diffraction pattern of the polycrystalline samples indicates single-phase $ThCr_2Si_2$-type structure with less than a few percent impurity phases. The low-field magnetization was measured in a 5 T MPMS system. The specific heat was measured in a PPMS

system over the temperature range between 1.8 and 300 K. Ceramic samples of about 6-8 mg were placed on the platform with Apiezon N-grease. The random fluctuations were verified through repeated measurements and are presented as error bars when they are larger than the symbol size in the figures.

Results and discussion

A literature survey of the specific heat data has been carried out. Almost all raw C_p / T data of $Ba_{0.6}K_{0.4}Fe_2As_2$ are in good agreement, but the extracted C_e / T and the conclusions drawn are very different, *i.e.* the result is mainly affected by the phonon baseline adopted.[3,9] This is especially noticeable in the low-T tail: the C_e / T is practically zero below 7 K $\approx T_c / 5$ in Ref. 3 but accounts for almost one-third of the overall C_p / T in Ref. 9 even though both have almost the same C_p / T.

Three procedures are typically used to extract C_{ph} / T: model fitting based on an assumed Debye-Einstein phonon-distributions;[3,5] referring to the C_p / T of some non-superconducting sibling compounds (with possible minor corrections);[9] or using the high-field C_p / T data. While the third method is difficult with the extremely high H_{c2} of $Ba_{0.6}K_{0.4}Fe_2As_2$, the first two routes have been widely adopted. Most works claiming a single-gap pairing adopted model fitting but those observing two-gap features utilized the C_{ph} / T of a sibling compound. To further explore the issue, the $Sr_{1-x}K_xFe_2As_2$ system was investigated first.

The evolution from the spin-density-wave state of $SrFe_2As_2$ to the superconductivity of $Sr_{0.55}K_{0.45}Fe_2As_2$ has been documented,[10] in addition to the normal-state C_p / T of the two materials.[8] To explore the issue, the data from $Sr_{0.55}K_{0.45}Fe_2As_2$ ceramic samples were analyzed. The measurements are repeatable to within a few mJ / mol K^2, with sample-to-sample variations only slightly larger. The C_{ph} / T was first modeled as $A_D\Phi_D(T / T_D) + (15R / T - A_D)\Phi_E(T / T_E)$, where A_D, Φ_D, Φ_E, T_D, T_E, and R are the Debye-phonon strength, Debye function, Einstein function, Debye temperature, Einstein temperature, and gas constant, respectively.[8] The carrier part C_e / T above T_c was represented by a T-independent constant γ up to 300 K, which is justified by the observation that the extracted high-T limit γ_H equals the low-T limit γ_L in this particular compound.[8] The fitting is rather stable and the fitting deviations are only slightly larger than the data fluctuation (Fig. 1a). The fitting parameters, $T_D = 204$ K, $T_E = 367$ K, $A_D = 69$, and $\gamma = 37\ \text{mJ / mol K}^2$, also appear to be reasonable. It should be pointed out that such good agreement is rare. The phonon contributions at both low-T and high-T limits are highly constrained, *i.e.* being zero and $15R / T$ respectively. A significant T-dependence of the carrier contribution (*e.g.* a variation of 10 mJ / mol K^2 or larger), therefore, will directly invalidate the model used. Such a situation, for example, occurs for both the non-superconducting $SrFe_2As_2$ with its $\gamma_L \approx 12$ and $\gamma_H \approx 54\ \text{mJ / mol K}^2$ and the superconducting $Ba_{0.6}K_{0.4}Fe_2As_2$ (the details of which will be addressed below).

To further examine the low-T parts, the raw data of $Sr_{0.55}K_{0.45}Fe_2As_2$ and its fitting result, as well as those of the non-superconducting $SrFe_2As_2$, are shown in Fig. 1b as $C_p / T - \gamma_0$ vs. T^2 plots, where γ_0 is the extrapolated zero-temperature limit. The fitting result of $Sr_{0.55}K_{0.45}Fe_2As_2$

increases linearly with T^2 up to 15 K (dashed red line in Fig. 1b) with a downward bend at higher temperatures (not within the figure's range). This is expected from the Debye function $\Phi_D(T/T_D) \propto (T/T_D)^2 - (T/T_D)^4/12 + \ldots$ and the Einstein function $\propto e^{T_E/T}/(e^{T_E/T}-1)^2$ with the high T_D and T_E values extracted. The Debye function produces a noticeable sublinearity only above $0.05T_D$, and the Einstein function is practically zero below $0.05T_E$ but shows superlinearity at slightly higher temperatures. The sublinearity of the fitting result, *e.g.* 0.03 J / mol K^2 lower than the linear extrapolation around 20 K, reflects the domination of the Debye component below $0.05T_E \approx 20$ K. This seems to be a common characteristic of most phonon models. The trend, however, should be violated if the phonon distribution deviates from the Debye model. The fitting result for $SrFe_2As_2$ is very similar (solid black line in Fig. 1b). The observed $C_p/T - \gamma_0$ data of $SrFe_2As_2$ (inverted black triangles in Fig. 1b), however, deviate from this expected linear T^2 dependency with a broad bump below 8 K. A slightly non-Debye distribution is suggested. Fortunately, the excess C_{ph}/T (≈ 3 mJ / mol K^2 at 5 K) is not large enough to affect the main conclusion. For $Sr_{0.55}K_{0.45}Fe_2As_2$, the $C_p/T = C_e/T + C_{ph}/T$ is almost overlapped with the C_{ph}/T of $SrFe_2As_2$ below 3 K $\approx 0.1kT_c$. Actually, the initial slopes $\beta = \dfrac{d(C_p/T)}{d(T^2)} = 7.3\cdot10^{-4}$ and $7.2\cdot10^{-4}$ J / mol K^4 for $Sr_{0.55}K_{0.45}Fe_2As_2$ and $SrFe_2As_2$, respectively, are within the data fluctuation. This may not be a pure coincidence. If the pairing in $Sr_{0.55}K_{0.45}Fe_2As_2$ is *s*-wave in nature and not affected by possible gaps narrower than $0.4kT_c$, the C_e/T should be negligibly small below 3 K. The raw data below 3 K, therefore, may tentatively be regarded as C_{ph}/T. It should be pointed out that, while our temperature range and the data accuracy might not totally exclude possible gap nodes, the assumptions are consistent with most

data reported so far. Above 5 K $\approx 0.15kT_c$, the $C_p/T-\gamma_0$ of $Sr_{0.55}K_{0.45}Fe_2As_2$ is systematically higher than that of $SrFe_2As_2$. An extensive low-T tail of C_e/T is unavoidable if the C_{ph}/T is x-insensitive. The data above $T_c \approx 35$ K, therefore, are compared. The result does support the assumption (inset, Fig. 1b).

Several procedures have been previously proposed to match the C_{ph}/T of sibling compounds: Loram et al. have expressed the C_{ph}/T evolution with the oxygen stoichiometry x for $YBa_2Cu_3O_{6+x}$ as a histogram of several discrete phonons. Based on the linear correlation observed between the amplitude of the modified phonons and the x value, the corrections are straightforward.[11] The method, however, apparently faces difficulties in the case of $Ba_{1-x}K_xFe_2As_2$. For example, the identified C_{ph}/T shifts against the parent compound $BaFe_2As_2$ vary with the x value non-linearly.[12] The approach, therefore, may not be useful in current case. The second procedure is a scaling approach, which is essentially an extrapolation from the C_{ph}/T above T_c based on the $C_{ph,1}/T$ of a non-superconducting sibling compound.[9] A scaling correlation of $AC_{ph,1}(BT)/(BT)=C_{ph}(T)/(T)$ is proposed between these sibling compounds where A and B are two adjustable parameters. It, however, will be a poor one if an x-dependent deviation from Debye distribution occurs below T_c, *e.g.* the x-dependent C_{ph}/T bump around 40 K in $YBa_2Cu_3O_{6+x}$.[11] This scaling algebra, in our view, can be significantly improved and possesses a self-verification ability if $C_e/T=\gamma_0$ below 3 K as argued above. The scaling procedure in such a case can be carried out both above T_c and below $0.1T_c \approx 3$ K. The C_{ph}/T in the superconducting state, therefore, can be easily *interpolated* between the two

regions if the two separated regions share the same parameters A and B. The procedure may also offer a way to verify the possible uncertainties. We propose that the possible distortions should be on the same order as the changes caused by the parameter variations. In the case of the $Sr_{0.55}K_{0.45}Fe_2As_2$-$SrFe_2As_2$ pair, for example, the scale fitting leads to $A = 1.042(8)$ and $B = 1.003(2)$ below 3 K, but $A = 0.950(2)$ and $B = 1.034(2)$ between 35 and 65 K (Fig. 1b). The phonon baseline of $Sr_{0.55}K_{0.45}Fe_2As_2$ between 3 K and T_c, therefore, should be within the calculated $AC_{ph,1}(BT)/(BT)$ spread over $0.95 < A < 1.04$ and $1 < B < 1.03$, where $C_{ph,1}$ is the phonon contribution in $SrFe_2As_2$.

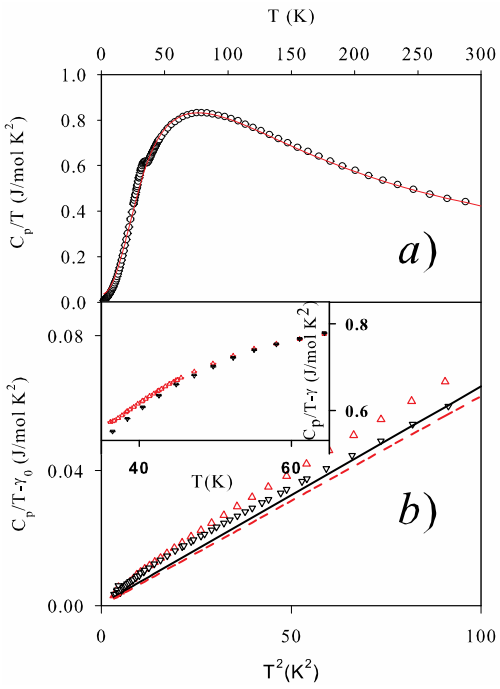

Figure 1: a) the model fit of the C_p / T for a $Sr_{0.55}K_{0.45}Fe_2As_2$ ceramic sample. Circles: the data; red line: the fit. b) $C_p / T - \gamma_0$ *vs* T^2 below 10 K. Red triangles: $Sr_{0.55}K_{0.45}Fe_2As_2$; inverted black triangles: $SrFe_2As_2$; solid black line: model fit of $SrFe_2As_2$; dashed red line: model fit of

$Sr_{0.55}K_{0.45}Fe_2As_2$. Inset: $C_p / T - \gamma$ of $SrFe_2As_2$ (inverted black triangles) and $Sr_{0.55}K_{0.45}Fe_2As_2$ (red triangles).

The average parameters of $A = 1$ and $B = 1.02$ are used to estimate the most likely C_e / T of $Sr_{0.55}K_{0.45}Fe_2As_2$ using the scaled C_{ph} / T of $SrFe_2As_2$ as the phonon baseline (inverted red triangles in Fig. 2a). The range of $0.95 < A < 1.04$ and $1 < B < 1.03$, on the other hand, is used to estimate the possible C_e / T spread (grey band in Fig. 2a). It is interesting to note that the C_p / T split between $SrFe_2As_2$ and $Sr_{0.55}K_{0.45}Fe_2As_2$, *e.g.* a $C_e / T \approx 8$ mJ / mol K^2 at 10 K $\approx 0.29 T_c$, is so large that a $\pm 5\%$ variation of the C_{ph} / T, *i.e.* ± 3 mJ / mol K^2, may not affect the overall character of the $\Delta C_p / T(\gamma - \gamma_0)$ tail. The C_e / T from the model fitting is also plotted (blue triangles). The two are in good agreement above 5K, but are significantly different at lower temperatures, which we interpreted as the result of non-Debye phonon-distribution below 3-5 K in $Sr_{0.55}K_{0.45}Fe_2As_2$. The $\gamma - \gamma_0 = 0.035$ mJ / mol K^2 and $\gamma_0 = 3$ mJ / mol K^2 of $Sr_{0.55}K_{0.45}Fe_2As_2$ based on the conservation of the carrier entropy (which will be further discussed below) is also in good agreement with the model fitting result of $\gamma = 37$ mJ / mol K^2 (Fig. 1).

The single-gap and two-gap α-model fits were subsequently carried out. It is known that both the $\Delta C_p / T(\gamma - \gamma_0)$ and the associated entropy of a single-gap *s*-wave BCS superconductor can be easily calculated based on a single parameter, the coupling strength $\alpha = 2\Delta / k_B T_c$, where $\Delta C_p = C_p - C_n$, and C_n is the extracted normal state specific heat.[13] It is further proposed that the $\Delta C_p / T(\gamma - \gamma_0)$ of a two-gap *s*-wave BCS superconductor will be a simple sum of $[r\Delta C_p(\alpha_1) + (1-r)\Delta C_p(\alpha_2)]/T(\gamma - \gamma_0)$, where *r*, α_1, and α_2 are the mixing ratio and the coupling strengths

respectively.[14] A non-linear least-square-fitting algebra has been adopted with r, α_1, and α_2 as free fitting parameters.[15] The best single-gap fitting, *i.e.* with a coupling strength $\alpha = 4.5$, fails to reproduce the tail observed (thin black line in Fig. 2a). Two-gap pairing, on the other hand, nicely reproduces the $\Delta C_p / T(\gamma - \gamma_0)$ of $Sr_{0.55}K_{0.45}Fe_2As_2$ with two gaps of $\Delta_1 = 2.6kT_c$ and $\Delta_2 = 0.5kT_c$, *i.e.* the coupling strengths $\alpha_1 = 5.2$ and $\alpha_2 = 1.0$, under a mixing ratio of 0.75 (thick red line in Fig. 2a). The distinction between single-gap and two-gap configurations can actually be viewed intuitively. Both the $\Delta C_p / T(\gamma - \gamma_0)$ jump at T_c and the low-T tail, *e.g.* the reduced temperature $t_{20\%} = T_{20\%} / T_c$, where the unpaired carriers account for $0.2(\gamma - \gamma_0)$ at $T_{20\%}$,[16] depend on the same parameter, *i.e.* the coupling strength $\alpha = 2\Delta_0 / kT_c$. Therefore, all single-gap configurations trace a curve in the two dimensional $t_{20\%}$ *vs.* $\Delta C_p / T(\gamma - \gamma_0)\big|_{T_c}$ phase space (thick line in Fig. 2b). The selection of 20% is largely a balance between the data resolution and the distinction over the two configurations. At lower percentage the data noise will be a problem, but the single-gap and two-gap configurations may predict a similar C_e / T at higher percentage. The deduced data of the $Sr_{0.55}K_{0.45}Fe_2As_2$ sample are shown in Fig. 2b using either the model fitting (solid red triangle) or scaled C_{ph} / T of $SrFe_2As_2$ as the phonon baseline (inverted solid red triangle). The vertical error bar on the inverted triangle corresponds to the variation associated with the two sets of the scale factors. The horizontal bar accounts for the variation over the raw jump-amplitude and that after extrapolation (*i.e.* the tip of the thick red and dashed black lines in Fig. 2a). The extracted parameters are collected in Table 1. It seems that the C_e / T character of $Sr_{0.55}K_{0.45}Fe_2As_2$ can hardly be associated with a single-gap pairing.

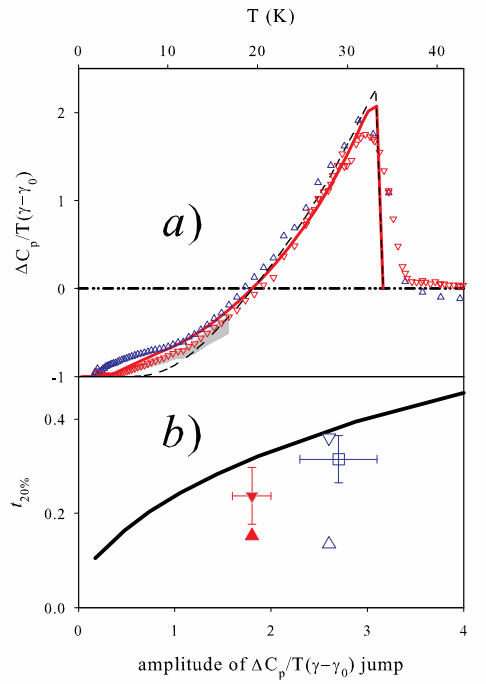

Figure 2. a) The deduced $\Delta C_p / T(\gamma-\gamma_0)$ of a ceramic $Sr_{0.55}K_{0.45}Fe_2As_2$ sample (see text). Blue triangles: from model; inverted red triangles: from the scaled C_p / T of $SrFe_2As_2$; grey band: the area covered by the variation in the scale factors; dashed black line: the optimal fit of single gap; thick red line: the optimal fit of two-gap configuration. b) The proposed phase diagram $t_{20\%}$ vs. $\Delta C_p / T(\gamma-\gamma_0)$ jump. Solid red triangle: from model fit of $Sr_{0.55}K_{0.45}Fe_2As_2$; inverted solid red triangle: $Sr_{0.55}K_{0.45}Fe_2As_2$ using the scaled C_p / T of $SrFe_2As_2$ as phonon background; Inverted open blue triangle: from model fit of $Ba_{0.6}K_{0.4}Fe_2As_2$; open blue triangle: $Ba_{0.6}K_{0.4}Fe_2As_2$ using the scaled C_p / T of $BaFe_2As_2$ as phonon background; blue open square: $Ba_{0.6}K_{0.4}Fe_2As_2$ result obtained here; thick line: the single-gap trace.

Table 1, The extracted parameters for $Sr_{0.55}K_{0.45}Fe_2As_2$ and $Ba_{0.6}K_{0.4}Fe_2As_2$

	$Sr_{0.55}K_{0.45}Fe_2As_2$	$Ba_{0.6}K_{0.4}Fe_2As_2$

γ	37 mJ/molK^2	47 mJ/molK^2
γ_0	3 mJ/molK^2	2 mJ/molK^2
α_1	5.1	6.0
α_2	1.0	2.4
r	0.75:0.25	0.75:0.25
$t_{20\%}$	0.15-0.24	0.13-0.36

The situation of $Ba_{0.6}K_{0.4}Fe_2As_2$ is much more complicated. To simply extract the γ value in the model fitting presents a challenge. Even after setting the entropy constraint and a heavy weight on the low-T part, the fit results in an unreasonably small $\gamma = 10$ mJ / mol K^2. The mean-square-deviation increases by more than a hundred times with γ varying from 10 to 60 mJ / mol K^2. The corresponding C_e / T between 5 and 15 K, however, is negative if $\gamma < 40$ mJ / mol K^2 (the bottom plot in inset, Fig. 3a). In fact, a broad dip around 10 K persists until $\gamma > 50$ mJ / mol K^2. Assuming a positive $d(C_e / T) / dT$ below T_c, a $\gamma = 60$ mJ / mol K^2 can be adopted with a rather large uncertainty (top plot, inset, Fig. 3a). Similar difficulties might be common, and the γ value has to be pre-fixed in some cases.[1] This seems to be a direct result of a rather low γ_H of $Ba_{0.6}K_{0.4}Fe_2As_2$, as suggested by the deviations above 200 K in Fig. 3a.

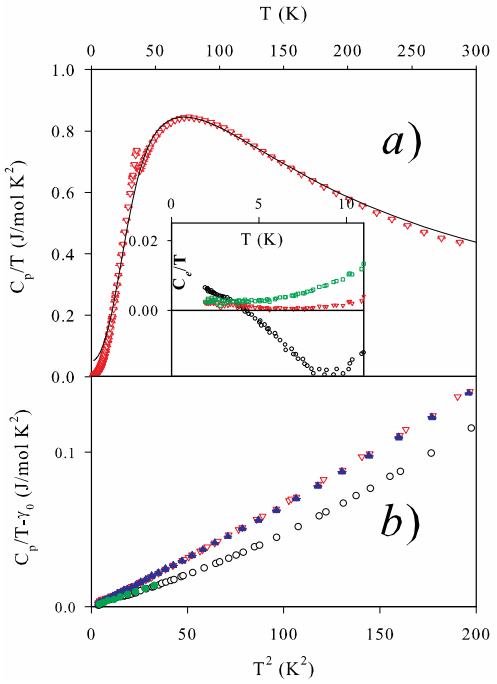

Figure 3. a) C_p / T vs. T of a ceramic $Ba_{0.6}K_{0.4}Fe_2As_2$ sample. $\gamma = 60$ mJ / mol K^2 is fixed. Inverted red triangles: data; black line: fit. Inset: the low-T part of the deduced carrier contribution C_e / T at $\gamma = 60$, 40 and 10 mJ / mol K^2 from top to bottom. b) $C_p / T - \gamma_0$ vs T^2 observed for $BaFe_2As_2$ (open black circles), $Ba_{0.6}K_{0.4}Fe_2As_2$ (open inverted red triangles), $Ba_{0.6}K_{0.4}(Fe_{0.9}Co_{0.1})_2As_2$ (solid blue triangles), and the reported $Ba(Fe_{0.88}Mn_{0.12})_2As_2$ (solid green circles).

An even more severe problem is the potential for shifts of the soft phonons with K-Ba replacement. This is obvious in the $C_p / T - \gamma_0$ *vs.* T^2 plots of Fig. 3b. Three non-superconducting sibling compounds of $BaFe_2As_2$, $Ba_{0.6}K_{0.4}(Fe_{0.9}Co_{0.1})_2As_2$, and $Ba(Fe_{0.88}Mn_{0.12})_2As_2$ (data from Ref. 7) are compared (Fig. 3b). The deduced $C_p / T - \gamma_0$ should represent the C_{ph} / T under the reasonable assumption that the C_e / T is T-independent at such low temperatures. Therefore, it is expected that either all plots overlap or they spread randomly

and narrowly. The three plots, however, roughly separate into two distinguishable groups with the initial slopes $\beta \approx 6 \cdot 10^{-4}$ J / mol K^4 for $Ba_{0.6}K_{0.4}(Fe_{0.9}Co_{0.1})_2As_2$, but $4 \cdot 10^{-4}$ J / mol K^4 for both $BaFe_2As_2$ and $Ba(Fe_{0.88}Mn_{0.12})_2As_2$. Above 20-30 K, however, the three share a common slope of $\frac{d(C_p / T)}{d(T^2)} \approx 4 \cdot 10^{-4}$ J / mol K^4. A prompt dip appears in $BaFe_2As_2$ over 5-15 K, which strongly suggests a depletion of soft phonons. In fact, the normal state $\gamma \approx 12$ mJ / mol K^2 of $BaFe_2As_2$ is far too small to account for the dip, ≈ 20 mJ / mol K^2 at 15 K. To exclude possible sample-quality problems, several ceramic samples as well as a few $BaFe_2As_2$ single crystals grown by self-flux were measured, with essentially the same results. A careful survey further shows that similar features also appear in most published data. It should be pointed out that the proposed scaling correction can hardly accommodate the difference between the C_{ph} / T s of $BaFe_2As_2$ and $Ba_{0.6}K_{0.4}(Fe_{0.9}Co_{0.1})_2As_2$. The two have very different curvatures in the C_{ph} / T vs. T^2 plots. The data will demand a ratio $A / B^2 \approx 1.5$ below 3 K, but $A \approx B \approx 1$ above T_c, two constraints that are hard to accommodate. Consequently, a natural question will be which dopants, Co or K, dominate the shifts of soft-phonons. For clarification, the $C_p / T - \gamma_0$ of the superconducting $Ba_{0.6}K_{0.4}Fe_2As_2$ is added (Fig. 3b). It is almost identical to that of $Ba_{0.6}K_{0.4}(Fe_{0.9}Co_{0.1})_2As_2$ below 3 K. This agreement is highly suggestive, especially considering the similar pair of $SrFe_2As_2$ and $Sr_{0.55}K_{0.45}Fe_2As_2$ (Fig. 1b). The K-Ba replacement, therefore, significantly shifts the phonon baseline at low- T, but the effects of both the Co-Fe and the Sr-K replacements are limited. A major factor is the differences in the ion weights. The replacement of the heavy Ba-ions by the much lighter K-ions is expected to significantly disturb the soft phonons.

The proposed effects of K-Ba replacement are actually supported by many previous reports. Storey *et al*. reported that the differential C_p / T between $BaFe_2As_2$ and $Ba_{0.9}K_{0.1}Fe_2As_2$ shows a broad "dip" of 20-30 $mJ / mol\ K^2$ over 10-40 K and attributed it to the shift in the phonon spectrum.[12] Lee *et al*. described a noticeable change of the soft phonons around 5-20 meV with x in $Ba_{1-x}K_xFe_2As_2$ through inelastic X-ray scattering.[17] Both are in line with above observations.

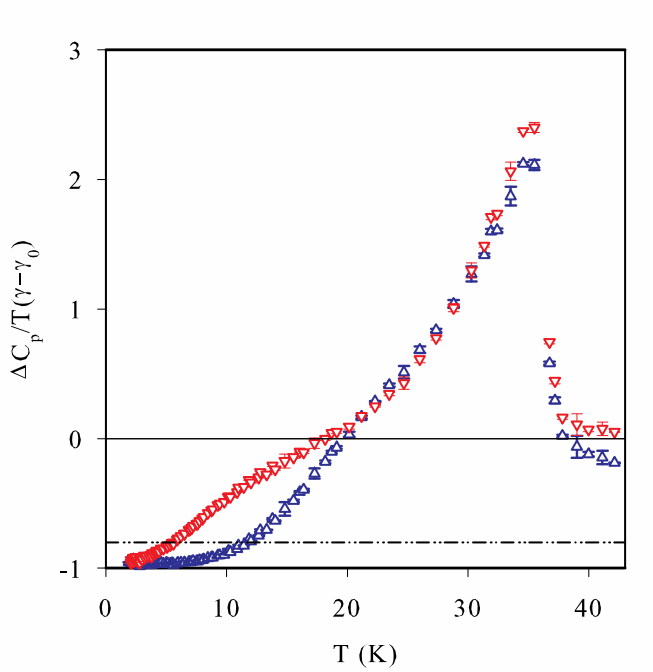

Figure 4. The deduced superconducting anomaly of a $Ba_{0.6}K_{0.4}Fe_2As_2$ ceramic sample based on the phonon baselines from model fitting (blue triangles) and the scaled $C_p / T - \gamma$ of $BaFe_2As_2$ (inverted red triangles). The horizontal dot-dashed line represents 20% uncondensed pairs.

The C_{ph} / T shift with K-Ba replacement may explain the controversial conclusions previously reported about the gap structure of $Ba_{0.6}K_{0.4}Fe_2As_2$. To reproduce these different results, two $\Delta C_p / T(\gamma - \gamma_0)$ sets were extracted from the same C_p / T of a $Ba_{0.6}K_{0.4}Fe_2As_2$ sample using the

C_{ph}/T of $BaFe_2As_2$ and model fitting, respectively (Fig. 4). The scaling factors from the fitting above T_c, *i.e.* $A = 0.95$ and $B = 1.03$, are almost the same as those of Ref. 9. It is interesting to note that the two sets nicely reproduce the results of Refs. 3 and 9, respectively. The 10 K dip in the C_{ph}/T of $BaFe_2As_2$ seems to play a significant role for the result reported previously. Such strong effects of K-Ba replacement stimulates our investigation of $Ba_{0.6}K_{0.4}(Fe_{1-y}Co_y)_2As_2$ with the hope that the soft phonons may be less sensitive to this Fe-site replacement as suggested by the same initial β of both $BaFe_2As_2$ and $Ba(Fe_{0.88}Mn_{0.12})_2As_2$.

The specific heat C_p and magnetization of several ceramic $Ba_{0.6}K_{0.4}(Fe_{1-y}Co_y)_2As_2$ samples with $y = 0$, 0.04, 0.08, and 0.1 were measured. The 10 Oe zero-field-cooled shielding χ_{ZFC} is shown in Fig. 5. The shielding is perfect, *i.e.* with $-4\pi\chi_{ZFC} > 1$, at $y \le 0.04$. However, it drops drastically with y, reaches $-4\pi\chi_{ZFC} < 0.2$ at $y = 0.085$, and disappears at $y = 0.1$. The $C_p/T - \gamma_0$ of the $y = 0.1$ sample, therefore, is taken as its phonon baseline C_{ph}/T, *i.e.* assuming the carrier contribution C_e/T is independent of T, at least below 50 K, where $\gamma_0 = 15$ mJ / mol K^2 is the zero-temperature limit of the C_p/T. The doping effects are then investigated by using the C_{ph}/T of the $y = 0.1$ sample as the reference line.

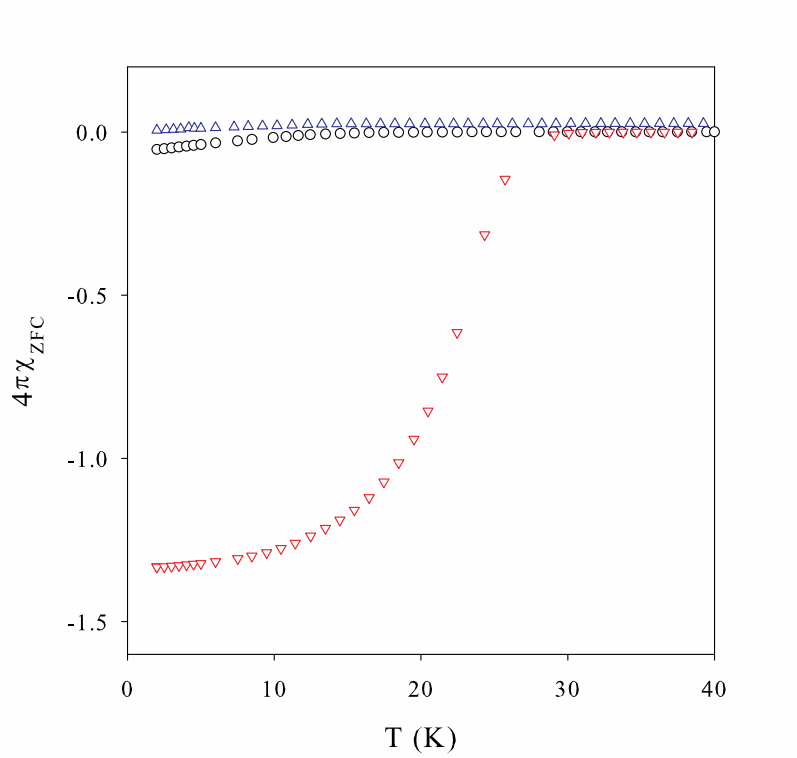

Figure 5. The 10 Oe zero-field-cooled magnetization of $Ba_{0.6}K_{0.4}(Fe_{1-y}Co_y)_2As_2$ with $y = 0.04$ (inverted red triangles), 0.085 (black circles), and 0.1 (blue triangles).

The same procedure used in the $Sr_{1-x}K_xFe_2As_2$ system was adopted for the $Ba_{0.6}K_{0.4}(Fe_{1-y}Co_y)_2As_2$ samples. The normal-state γ was first roughly estimated through model fitting. The corresponding C_{ph}/T, *i.e.* $C_p/T-\gamma$ above T_c and $C_p/T-\gamma_0$ below 3 K, of $Ba_{0.6}K_{0.4}(Fe_{0.915}Co_{0.085})_2As_2$ and $Ba_{0.6}K_{0.4}(Fe_{0.9}Co_{0.1})_2As_2$ is shown in Fig. 6a. A quick check suggests that the data of the two compounds have rather similar T-dependencies. $A = 0.917(7)$ and $B = B = 0.992(6)$ are then obtained over $T_c \approx 22$ K up to 40 K at an assumed $\gamma = 0.025$ J / mol K^2 for the $y = 0.085$ sample. Below 3 K, a similar fit leads to $A = 0.98(4)$ and

$B = 1.02(2)$. The scaled data are in good agreement and the parameters at the two separated regions differ only slightly. In particular, $B = 1$ within the fitting uncertainties.

The fitting, however, still depends on the adopted γ value. A regression procedure, therefore, is used to make sure the result is reasonable and at least self-consistent. This is because both the C_e / T and the S / T associated with the scaled C_{ph} / T strongly depend on the parameters. The C_e / T and the entropy S / T of the carrier section associated with two different A values of 0.917 (red line) and 0.927 (black line), for example, are plotted in Fig. 6b. The entropy conservation of $\int_0^{T>T_c} \frac{C_e}{T'} dT' = \gamma T$, however, demands $C_e / T = S / T$ above T_c. The data, however, confirm that the split C_e / T - S / T is a strong function of the scaling parameters. A regression may easily lead to a self-consistent solution, *i.e.* $A = 0.917$, $B = 1$, and $\gamma = 0.025$ J / mol K^2 in the case of $y = 0.085$.

It should be pointed out that the $y = 0.085$ sample is an interesting case. The weak low-field screening of $4\pi\chi\big|_{5\text{ K}} \approx -0.2$ and the larger ratio $\gamma_0 / \gamma \approx 0.5$, both of which should indicate the same superconducting volume fraction, are in disagreement. The average T_c suggested by the two probes, *i.e.* < 10 K from the $4\pi\chi_{ZFC}$ but > 20 K from the C_e / T, also differs significantly. All of these may be indications of mesoscopic phase-separation.[18]

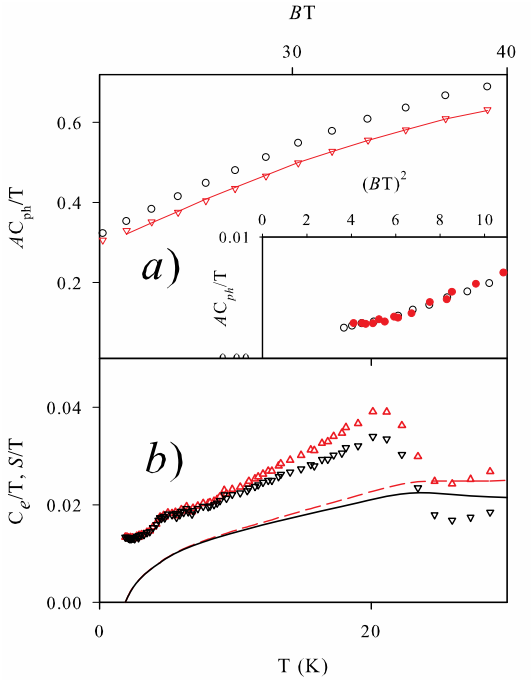

Figure 6. a) The $C_p(T)/T-\gamma$ *vs* BT, *i.e.* with $A=B=1$, above T_c for a $Ba_{0.6}K_{0.4}(Fe_{0.915}Co_{0.085})_2As_2$ sample (red triangles) and a $Ba_{0.6}K_{0.4}(Fe_{0.9}Co_{0.1})_2As_2$ sample (black circles). The solid red line is the scaled $A[C_p(BT)/BT-\gamma_0]$ data of the $Ba_{0.6}K_{0.4}(Fe_{0.9}Co_{0.1})_2As_2$ with $A=0.917$ and $B=0.992$. Inset: the $C_p(T)/T-\gamma_0$ of the $Ba_{0.6}K_{0.4}(Fe_{0.915}Co_{0.085})_2As_2$ sample (solid red circles) and the scaled $A[C_p(BT)/BT-\gamma_0]$ of the $Ba_{0.6}K_{0.4}(Fe_{0.9}Co_{0.1})_2As_2$ sample (open black circles, $A=0.98$ and $B=1.02$) below 3 K. b) The regression results of C_e/T (red triangles) and S/T (dashed red line) for a ceramic $Ba_{0.6}K_{0.4}(Fe_{0.915}Co_{0.085})_2As_2$ sample. The black inverted triangles and line are with a scale factor 1% higher.

Finally, both the scaling approximation and the γ regression were used to calculate the C_e/T of the $Ba_{0.6}K_{0.4}Fe_2As_2$ sample based on the $C_{ph}/T=C_p/T-\gamma_0$ of $Ba_{0.6}K_{0.4}(Fe_{0.9}Co_{0.1})_2As_2$. The deduced $A\cdot C_{ph}(B\cdot T)/(B\cdot T)$ perfectly matches the normal state $C_p/T-\gamma$ of $Ba_{0.6}K_{0.4}Fe_2As_2$

over 37-80 K with the scaling factors $A = 0.934(1)$ and $B = 0.981(1)$ together with a self-consistent $\gamma = 0.046$ J / mol K^2 (Fig. 7). Below 3 K, the fitting parameters $A = 0.93(2)$ and $B = 1.02(1)$ with $\gamma_0 = 0.015$ and 0.002 J / mol K^2 for $Ba_{0.6}K_{0.4}(Fe_{0.9}Co_{0.1})_2As_2$ and $Ba_{0.6}K_{0.4}Fe_2As_2$, respectively (inset, Fig. 7). The spread of the scaling parameters is relatively narrow and demonstrates that the phonon spectrum is insensitive to the Co-Fe replacement. This is in great contrast to the case of the $Ba_{0.6}K_{0.4}Fe_2As_2$-$BaFe_2As_2$ pair, where the value of A, for example, may vary from ≈ 1 above T_c to ≈ 1.5 below 3 K.

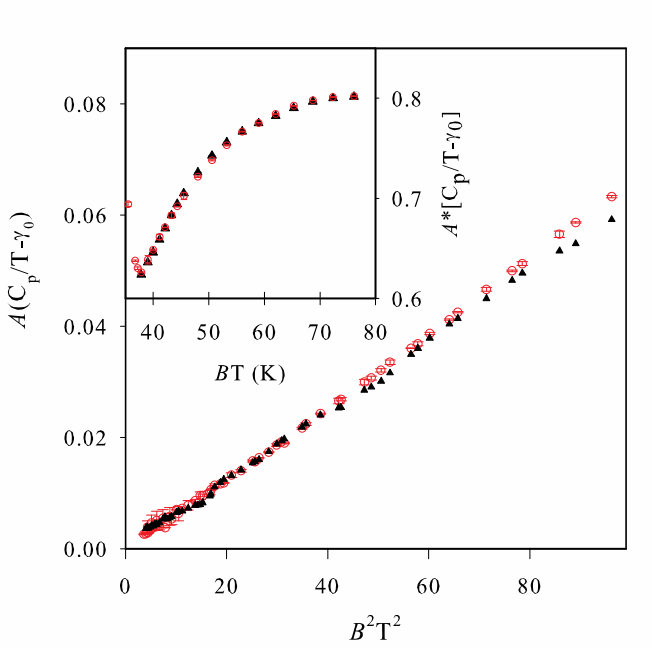

Figure 7. The scaled $A[C_p(BT)/BT - \gamma_0]$ *vs.* $(BT)^2$ below 10 K for $Ba_{0.6}K_{0.4}Fe_2As_2$ (open red circles, $A = B = 1$) and $Ba_{0.6}K_{0.4}(Fe_{0.9}Co_{0.1})_2As_2$ (solid black triangles, $A = 0.93$ and $B = 1.02$). Inset: The scaled $A[C_p(BT)/BT - \gamma_0]$ *vs.* BT between T_c and 80 K for $Ba_{0.6}K_{0.4}Fe_2As_2$ (open red circles, $A = B = 1$) and $Ba_{0.6}K_{0.4}(Fe_{0.9}Co_{0.1})_2As_2$ (solid black triangles, $A = 0.934$ and $B = 0.981$)

The C_e / T of $Ba_{0.6}K_{0.4}Fe_2As_2$ was then deduced (Fig. 8). The scaling parameters above T_c are used in the calculation of the "most likely" value, since those below 3 K possess much larger uncertainties. The resulting C_e / T has an obvious low-T tail (red triangles in Fig. 8), though far weaker than that reported in Ref. 9. The α-model fitting with single-gap and two-gap configurations prefers a two-gap configuration (Fig. 8). The optimal fitting parameters are: $\alpha = 5.2$ for the single-gap scenario, or $\alpha_1 = 6$, $\alpha_2 = 2.4$ at a mixing ratio of 0.75:0.25 for the two-gap configuration, where $\alpha = 2\Delta / kT_c$ is the coupling strength. To explore the resolution of the analysis, the C_e / T spread, which corresponds to variations of $0.93 \le A \le 0.94$ and $0.98 \le B \le 1.02$, is marked as the grey band in Fig. 8. Although the spread is noticeable, it cannot alter the main conclusion of a two-gap configuration. Single-gap configurations can hardly account for the extented tail below 12 K. This can also be seen clearly in Fig. 2b, where the horizontal error bars represent the uncertainty of the $\Delta C_p / T(\gamma - \gamma_0)$ jump, *i.e.* from the maximum of the raw data to the extrapolated tip, and the vertical bars cover the area of the grey band. The fitting results of $\alpha_1 \approx 6$ and $\alpha_2 \approx 2.4$ are in good agreement with reported ARPES data.[1,19] The extracted α_1 value seems to be in reasonable agreement with the results of Ref. 9 considering the ceramic nature of our samples. The thermodynamic weight of the narrower gap, *i.e.* $\approx 25\%$, however, is much lower than that of 50% reported. The α_2 value is also slightly higher. These are likely the results of the phonon backgrounds chosen.

It is interesting to compare $Ba_{0.6}K_{0.4}Fe_2As_2$ with $Sr_{0.55}K_{0.45}Fe_2As_2$. The extracted $t_{20\%}$ vs. $\Delta C_p / T$ data lie significantly below the single-gap trace in both cases as expected (Fig. 2b). The

two compounds seem to share similar two-gap structures, as suggested by their comparable distances to the single-gap trace. This may be related to the fitting result, which indicated that the two compounds share the same thermodynamic weights, *i.e.* $\approx 0.75:0.25$, associated with the two gaps. The α_1 value, *i.e.* 5-6, almost the same in both cases and far larger than the BCS value of 3.5, demonstrates a strong coupling strength. However, the raw data as well as the extracted α_1 and α_2 values consistently suggest larger couping strength in the Ba system.

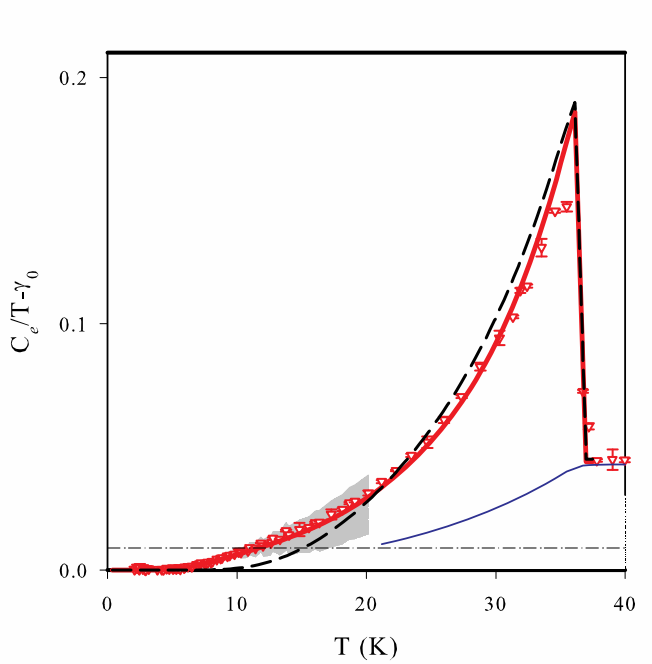

Figure 8. The $C_e/T-\gamma_0$ (red triangles) of a $Ba_{0.6}K_{0.4}Fe_2As_2$ sample using the scaled C_{ph}/T of a $Ba_{0.6}K_{0.4}(Fe_{0.9}Co_{0.1})_2As_2$ sample to extract the background. The grey area represents all possible $C_e/T-\gamma_0$ s while the scaling factors change from $A=0.934$ and $B=0.981$ to $A=0.93$ and $B=1.02$. The thin solid blue line is the corresponding S/T, which self-consistently determines the $\gamma=\gamma_0+0.045$ J / mol K^2. The horizontal dot-dashed black line marks $C_e/T=0.2(\gamma-\gamma_0)$.

The dashed black line is the best single-gap fit with $\alpha = 5.3$ and the thick solid red line is the two-gap result with $\alpha_1 = 6$ and $\alpha_2 = 2.4$ mixed with a ratio of 0.75:0.25.

The two-gap feature seems to be a well-established characteristic of $Ba_{0.6}K_{0.4}Fe_2As_2$, based on various microscopic probes, such as ARPES. Its appearance in the specific heat, however, is relatively marginal. One of the possible reasons might be the relative thermodynamic weights. In summary, the C_p / T of $M\mathrm{Fe}_2\mathrm{As}_2$ with $M =$ Ba and Sr has been investigated below T_c. The data suggest that the previous controversy surrounding the gap structure mainly arises from the treatment of the phonon background. In particular, the C_{ph} / T distortion created by the K-Ba replacement may be large enough to alter the inferred nature of the gap structure. By selecting the non-superconducting $(Ba_{0.6}K_{0.4})(Fe_{0.9}Co_{0.1})_2As_2$ as the reference compound and modifying the scaling approximation into an interpolation procedure, the C_e / T and its possible uncertainties are calculated for both $Ba_{0.6}K_{0.4}Fe_2As_2$ and $Sr_{0.55}K_{0.45}Fe_2As_2$. The data suggest a two-gap configuration in both cases, but that of $Ba_{0.6}K_{0.4}Fe_2As_2$ has a stronger coupling strength and a slightly higher T_c.

Acknowledgement

We thank Dr. J. Shulman for helpful discussions. The work in Houston is supported in part by AFOSR No. FA9550-09-1-0656, DoE subcontract 4000086706 through ORNL, AFRL subcontract R15901 (CONTACT) through Rice University, the T. L. L. Temple Foundation and TCSUH; and at LBNL by the Director, Office of Science, OBES, DMSE, DoE.

1. H. Ding, P. Richard , K Nakayama, K. Sugawara, T. Arakane, Y. Sekiba, A. Takayama, S. Souma, T. Sato, T. Takahashi, Z. Wang, X. Dai, Z. Fang, G. F. Chen, J. L. Luo and N. L. Wang, Europhys. Lett. 83, 47001(2008); K. Nakayama, T. Sato, P. Richard, Y.-M. Xu, Y. Sekiba, S. Souma, G. F. Chen, J. L. Luo, N. L. Wang, H. Ding and T. Takahashi, Europhys. Lett. 85, 67002 (2009).
2. R. S. Gonnelli, D. Daghero, M. Tortello, G. A. Ummarino, V. A. Stepanov, R. K. Kremer, J. S. Kim, N. D. Zhigadlo and J. Karpinski, Physica C, 469, 512 (2009).
3. G. Mu, H. Q. Luo, Z. S. Wang, L. Shan, C. Ren and H. H. Wen, Phys. Rev. B 79, 174501 (2009).
4. C. Ren, Z. S. Wang, H. Q. Luo, H. Yang, L. Shan and H. H. Wen, Phys. Rev. Lett. 101, 257006 (2008).
5. Ch. Kant, J. Deisenhofer, A. Günther, F. Schrettle, A. Loidl, M. Rotter and D. Johrendt, Phys. Rev. B 81, 014529 (2010).
6. F. Wei, F. Chen, K. Sasmal, B. Lv, Z. J. Tang, Y. Y. Xue, A. M. Guloy, and C. W. Chu, Phys. Rev. B 81, 134527 (2010).
7. F. Hardy, T. Wolf, R. A. Fisher, R. Eder, P. Schweiss, P. Adelmann, H. v. Löhneysen and C. Meingast, Phys. Rev. B 81, 060501(R) (2010).

8. F. Y. Wei, B. Lv, F. Chen, Y. Y. Xue, and C. W. Chu, Phys. Rev. B 83, 024503 (2011)

9. P. Popovich, A. V. Boris, O. V. Dolgov, A. A. Golubov, D. L. Sun, C. T. Lin, R. K. Kremer and B. Keimer, Phys. Rev. Lett. 105, 027003 (2010).

10. For example, K. Sasmal, B. Lv, B. Lorenz, A. M. Guloy, F. Chen, Y. Y. Xue and C. W. Chu, Phys. Rev. Lett. 101, 107007 (2008).

11. J. W. Loram, K. A. Mirza, J. R. Cooper and W. Y. Liang, Phys. Rev. Lett. 71, 1740 (1993).

12. J. G. Storey, J. W. Loram, J. R. Cooper, Z. Bukowski and J. Karpinski, arXiv1001.0474 [cond-mat.supr-con] (2010).

13. H. Padamsee, J. E. Neighbor and C. A. Shiffman, J. Low Temp. Phys. 12, 387 (1973).

14. F. Bouquet, Y. Wang, R. A. Fishe, D. G. Hinks, J. D. Jorgensen, A. Junod, N. E. Phillips, Europhys. Lett. 56, 856, 2001.

15. F. Wei, F. Chen, K. Sasmal, B. Lv, Z. J. Tang, Y. Y. Xue, A. M. Guloy and C.W. Chu, Phys. Rev. B, 81, 134527 (2010).

16. The choice of 20% uncondensed pairs (z) is a compromise between the experimental resolution and the ability to distinguish the single-gap configuration from the two-gap one. The difference among various configurations is more dramatic at lower z. The noise floor (around 1 mJ / mol K^2 over 5-10 K) and the uncertainty in the scale correction, however, make a $z < 10\%$ unfavorable.

17. C. H. Lee, K. Kihou, K. Horigane, S. Tsutsui, T. Fukuda, H. Eisaki, A. Iyo, H. Yamaguchi, A. Q. R. Baron, M. Braden and K. Yamada, Journal of the Physical Society of Japan 79, 014714 (2010).

18. F. Y. Wei, B. Lv, F. Chen, K. Sasmal, J. Shulman, Y. Y. Xue and C. W. Chu, Phys. Rev. B 83, 094517 (2011).

19. D. V. Evtushinsky, D. S. Inosov, V. B. Zabolotnyy, A. Koitzsch, M. Knupfer, B. Büchner, M. S. Viazovska, G. L. Sun, V. Hinkov, A. V. Boris, C. T. Lin, B. Keimer, A. Varykhalov, A. A. Kordyuk and S. V. Borisenko, Phys. Rev. B 79, 054517 (2009).